scientific reports

OPEN

FISH unveils a unified method for multi-marker biodose assessment

Rajesh Kumar Chaurasia[1], K. B. Shirsath[1], U. S. Mungse[1], N. N. Bhat[1,2], Arshad Khan[1] & B. K. Sapra[1,2✉]

Accurate dose assessment following radiation disasters or accidents is crucial for informed medical interventions. Cytogenetic biomarkers, such as dicentrics (dic), translocations, and chromosomal fragments, are essential for radiation biodosimetry in various exposure scenarios. However, quantifying these markers via separate staining and detection methods presents challenges in terms of efficiency and consistency. This study aimed to quantify multiple cytogenetic markers, including dic, balanced and unbalanced translocations and acentric fragments, from the same metaphases via fluorescence in situ hybridization (FISH). By enabling multimarker dose estimation from a single sample, this approach minimizes interexperimental variation and improves overall accuracy. Independent calibration curves were generated for each marker, enabling precise dose estimation with smaller class intervals, in accordance with the IAEA and ISO guidelines. The method was validated by estimating doses for five blinded samples via both standard cytogenetic methods and protein biomarkers (γH2AX and 53BP1). The multimarker approach yielded the closest estimates with 2–7% variation from true doses, providing the most accurate results among all cytogenetic techniques. This unified FISH-based approach enhances the precision of dose estimation for both recent and past radiation exposures, offering a more reliable tool for diverse biodosimetry applications.

The increasing use of ionizing radiation in healthcare, energy, industry, and research has increased the risk of overexposure in both occupational and nonoccupational settings[1]. Moreover, natural sources, such as cosmic rays and radon, contribute to unavoidable background radiation exposure[2]. The biological effects of ionizing radiation can be explained by three major models: linear threshold, linear no-threshold, and hormesis. Among these, the linear no-threshold (LNT) model is widely accepted and suggests that any level of radiation, however low, can induce harmful stochastic effects, such as gene mutations and cancer[3]. Therefore, the implementation of stringent radiation protection strategies is crucial. While these measures reduce radiation exposure, eliminating it entirely is impossible[4].

Physical dosimeters are the standard for measuring occupational radiation exposure, but they can be compromised under certain conditions, such as nonuniform exposure or mishandling by workers[5]. Biodosimetry, therefore, has become a critical tool in these cases, providing accurate estimates of radiation exposure and advancing our understanding of its impact on human health[6]. Various cytogenetic markers are employed for dose estimation, each of which is suited to different exposure scenarios and time points postexposure. Dicentrics, considered the gold standard, are limited by their instability over time[6–9]. In contrast, balanced translocations (BTs) persist throughout an individual's lifetime, as they do not involve the loss of genetic material and pass through cell cycle checkpoints[10,11]. Traditional detection techniques, such as Giemsa staining for dic (dic-G) and G-banding for translocations, are labor intensive and time consuming[6,7]. Currently, G-banding is seldom used for retrospective dosimetry due to its limitations. A unified approach to quantifying multiple cytogenetic markers from the same metaphase would streamline the process, reduce variability, and increase accuracy.

Recent advancements in chromosome-specific libraries have enabled the use of fluorescence in situ hybridization (FISH) for precise visualization of individual chromosomes, allowing the simultaneous detection of multiple markers, such as dic-F, unbalanced translocations (UT), balanced translocations (BT), and acentric fragments[12]. FISH not only simplifies translocation detection but also increases sensitivity by identifying aberrations that conventional banding methods might miss[6,13]. While G-banding can detect large-scale chromosomal changes (5–10 megabases), FISH offers superior resolution, detecting events (of a few kilobases) down to individual genes or smaller regions[14].

[1]Radiological Physics and Advisory Division, Bhabha Atomic Research Centre (BARC), Mumbai, India. [2]Homi Bhabha National Institute (HBNI), Mumbai, India. ✉email: bsapra@barc.gov.in

FISH also provides flexibility in genome coverage: two-color FISH (using chromosome pairs 1 and 2) covers 16.5% of the genome, three-color FISH (pairs 1, 2, and 4) covers 22.71%, and multiplex-FISH covers the entire genome[15]. Higher genome coverage leads to the detection of more cytogenetic markers, thus improving the precision of dose estimates[16]. However, increasing the number of cells scored can statistically strengthen the dataset and enhance the accuracy of dose estimates by reducing variability and improving result precision. This approach is particularly beneficial for achieving reliable dose assessments, especially at low-dose exposures, where statistical power plays an important role.

A core practice in biodosimetry labs is the establishment of dose−response curves (DRCs) for accurate dose estimation in suspected cases of radiation overexposure[6,7]. This study presents data on the development of ex vivo DRCs for ^{60}Co-γ-rays, using a unified two-color FISH method to quantify BT, UT, dic-F, and acentric-fragments in the same metaphases. Furthermore, we compared the performance of two-color, three-color, and multiplex-FISH to assess their relative effectiveness in improving dose estimation accuracy.

The DRCs were validated by estimating the radiation doses of five blinded samples via independent methods such as Giemsa staining for dic and micronuclei (MNs), immunofluorescence for γH2AX and 53BP1, and unified two-color FISH for BT, UT, dic-F, and acentric-fragments.

The Biodosimetry Laboratory at Bhabha Atomic Research Centre (BARC), Mumbai, which serves as India's central reference facility[17,18], will adopt the calibration curves generated in this study to standardize dose estimation in various radiation exposure scenarios across the country.

Materials and methods
Chemicals
RNase and DAPI (ProLong™ Diamond Antifade Mountant with DAPI) were obtained from Thermo Fisher Scientific and Invitrogen, USA. Tween 20, poly L-lysine, pepsin, BSA, L-glutamine, Giemsa, and Histopaque-1077 were obtained from Sigma−Aldrich, USA. RPMI 1640, paraformaldehyde, PHA, Triton X-100, FCS, HBSS, and colcemid were obtained from Gibco Life Technologies, USA. Chromosome paint probes were obtained from Metasystems, Germany. DPX was procured from Merck, USA. Rabbit anti-phospho 53BP1 monoclonal IgG and Texas red-labeled goat anti-rabbit IgG were obtained from CST, USA, and Invitrogen, USA.

Ethical approval, donor selection and blood collection
The study, approved by the Institutional Ethics Committee of the Bhabha Atomic Research Centre, involved three healthy male volunteers (aged 24, 30, 35) with no history of prior radiation exposure. A trained phlebotomist collected 7 ml of blood via heparinized vacutaiers. Ethical guidelines were followed strictly, with informed consent obtained from all participants.

Gamma irradiation, whole blood culture and chromosome preparation
Blood samples were divided into seven tubes and exposed to ^{60}Co-γ-rays at doses ranging from 0.0 to 4.0 Gy at 1 Gy/min. After irradiation, the samples were incubated at 37 °C with 5% CO_2 for 3 h to allow DNA repair. Two cultures per dose were established, totaling 42 cultures across three volunteers. Blood cultures were prepared following our own optimized protocol[19,20] with RPMI-1640, FCS, PHA, L-glutamine, and antibiotics. At 24 h, colcemid (100 μl of 250 μg/ml) was added to prevent a second cell division cycle[21]. The metaphases were harvested at 52 h with an automated system (HANABI P3 Plus Metaphase Chromosome Harvester, ADS Biotec, HCMH-99-003P, UK) after treatment with a hypotonic solution and Carnoy's fixative (3:1, methanol: acetic acid). Slides were prepared, treated with RNase, and stored at – 20 °C for further analysis.

Two-color fluorescence in situ hybridization (FISH)
One slide per dose point, containing over 2000 high-quality metaphases, was processed for FISH. Chromosomes 1 and 2 were hybridized via FITC- and Texas Red-labeled probes (Metasystems, Germany). Following slight modifications to the manufacturer's protocol[22], the slides were hydrated, treated with pepsin, and denatured. Probes were applied and hybridized overnight at 37 °C. After incubation, the slides were washed, dehydrated, and counterstained with DAPI for microscopic analysis. Similarly, three-color FISH was also performed.

Multiplex fluorescence in situ hybridization (mFISH)
Two slides exposed to 1 and 2 Gy doses were selected for 24-color mFISH via the Xcyting 24 Metasystems probe cocktail[23]. After rehydration, the slides were treated with pepsin, fixed with formaldehyde, and denatured in NaOH. Following dehydration, the denatured probe was applied and incubated for 3 days. After incubation, the slides were washed and subjected to three detection steps with streptavidin and anti-streptavidin. Finally, the slides were air dried, stained with DAPI, and cover-slipped for microscopic analysis.

Image acquisition and aberration assessment
Slides were scanned via an Axio Imager Z2 automated microscope (Carl Zeiss, Germany) equipped with ISIS, Ikaros, and Metafer5 software. Initial scans at 10× magnification identified high-quality metaphases, followed by final image captures at 63× magnification in AutoCapt mode. For two-color FISH, metaphases were captured under FITC, Texas Red, and DAPI filters, while mFISH required six filters: FITC, Spectrum Orange, Texas Red, Cy5, DEAC, and DAPI. Images were overlaid for analysis. Chromosomal analysis adhered to IAEA guidelines and other standards[6,7]. Whole-genome equivalent translocation frequencies were estimated via the Lucas formula[24].

$$F_G = \frac{F_{P(g+o)}}{2.05\left[f_g\left(1-f_g\right)+f_o\left(1-f_o\right)-\left(f_g f_o\right)\right]}$$

where F_G represents genome equivalence translocation frequencies, F_p signifies the translocation frequency determined by two-color FISH, f_g indicates the fraction of the genome covered by the green probe, and f_o represents the fraction of the genome covered by the orange probe.

Dose reconstruction of blinded samples by multiple assays

An anonymous volunteer (unrelated to calibration curve generation) participated in the validation. After providing informed consent, 15 ml of blood was drawn and split into five 3 ml samples. Peripheral blood mononuclear cells (PBMCs) were isolated from 1 ml of each sample via Histopaque-1077. Both whole blood and PBMCs were irradiated with blinded doses. Two sets of cultures were prepared per dose for metaphase analysis and the cytokinesis-block micronucleus (CBMN) assay via our own optimized protocol[19,20]. Over 1000 metaphases and binucleated cells were analyzed for dic-G and MN. Additionally, irradiated PBMCs were subjected to immunofluorescence staining to assess γH2AX and 53BP1 foci, one hour post-irradiation. Over 300 lymphocytes were analyzed for each radiation dose to ensure statistical robustness. The dose-response curve established at this time point was subsequently utilized for accurate dose estimation[17,18].

Doses were estimated for all the markers independently. Avg-FISH refers to the arithmetic mean (average) of the doses estimated independently via the markers BT, UT, dic-F, and fragments, each quantified from the same metaphases processed via FISH.

Statistical analysis

Assuming a Poisson distribution of aberrations, the standard error of the mean (SEM) was calculated via the Papworth U test, with the data expressed as the means ± SEMs. For each dose, the dispersion index (σ^2/Y) was expected to be close to one, and the Papworth U test (u test value) was within ± 1.96. A paired t test ($p=0.05$) was used to compare means. Dose uncertainties were addressed by calculating 95% confidence intervals per IAEA guidelines[7].

Results
Construction of a multimarker calibration curve via the single FISH method

Multiple cytogenetic markers, including BT, UT, dic-F and acentric fragments, were quantified from the same metaphases via two-color FISH. The aberration distribution among cells at each dose point was tested for compliance with the Poisson distribution, as curve fitting relies on Poisson statistics[25]. Tables 1, 2, 3 and 4 present the dispersion analysis results for all aberrations quantified from these metaphases. BT and UT exhibited compliance with the Poisson distribution across all seven dose points. dic-F adhered to the Poisson distribution at six dose points, except at 4 Gy, where underdispersion was observed. Similarly, acentric fragments followed the Poisson distribution at five dose points, with deviations in the form of overdispersion noted at 3 and 4 Gy. These observed deviations at higher doses are consistent with previous reports[6,7,19,20,26,27].

To construct the dose–response curves, different numbers of cells were scored for stable aberrations (BT) and unstable aberrations (UT, dic-F and acentric fragments). For stable aberrations, 1012, 1091, approximately 1036, 773, 766, 329, and 334 cells/individual were scored at dose points of 0, 0.25, 0.5, 1, 2, 3, and 4 Gy, respectively. For unstable aberrations, 1012, approximately 1153, 997, 887, 1532, 742, and 1117 cells/individual were scored at these same dose points. In scoring for stable aberrations, only cells with BT were counted, while cells containing other aberrations were excluded; hence, a lower cell count occurred at higher dose levels. The inclusion and exclusion criteria for stable and unstable aberrations were applied following the IAEA and ISO recommendations[6,7,24,28]. Figure 1 illustrates representative metaphases bearing stable and unstable aberrations that were considered in the analysis. The data generated (Tables 1, 2, 3 and 4) for dose–response curve construction is plotted in Fig. 2 (A-D). Regression analysis and data plotting were performed via OriginLab 2021 software[29]. The data for all types of aberrations were fitted via a linear–quadratic model following the expression $Y = C + \alpha D + \beta D^2$, where α and

Dose (Gy)	Cells scored	BT (No)	Distribution of balanced translocation (BT) D0	D1	D2	D3	Yield (Y)	Papworth u test (u test value)	Dispersion index (σ^2/Y)	Distribution
0	3036	0	3036	0	0	0	0	0	0	P
0.25	3273	16	3257	16	0	0	0.00489	– 0.19	1	P
0.5	3109	40	3069	40	0	0	0.01287	– 0.5	0.99	P
1	2318	69	2250	67	1	0	0.02977	– 0.01	1	P
2	2297	172	2129	164	4	0	0.07488	– 0.95	0.97	P
3	988	188	811	166	11	0	0.19028	– 1.61	0.93	P
4	1001	204	817	165	18	1	0.20386	0.07	1	P

Table 1. Yield and distribution of balanced translocations (BTs) involving painted chromosome pairs 1 and 2 following ex vivo irradiation ($n=3$) with 0–4 Gy of ^{60}Co-γ-rays. All datasets were in agreement with the Poisson distribution (P, u-test values were within the range of ± 1.96).

Dose (Gy)	Cells scored	UT (No)	Distribution of unbalanced translocation (UT)				Yield (Y)	Papworth u test (u test value)	Dispersion index (σ^2/Y)	Distribution
			D0	D1	D2	D3				
0	3036	1	3035	1	0	0	0.00033	− 0.01	1	P
0.25	3460	6	3454	6	0	0	0.00174	− 0.07	1	P
0.5	2990	6	2984	6	0	0	0.00201	− 0.07	1	P
1	2660	34	2626	34	0	0	0.01278	− 0.46	0.99	P
2	4596	155	4442	153	1	0	0.03373	− 0.99	0.98	P
3	2227	141	2088	137	2	0	0.06332	− 1.16	0.97	P
4	3350	453	2915	420	12	3	0.13523	− 1.73	0.96	P

Table 2. Yield and distribution of unbalanced translocations (UTs) involving painted chromosome pairs 1 and 2 following ex vivo irradiation ($n = 3$) with 0–4 Gy of ^{60}Co-γ-rays. All datasets were in agreement with the Poisson distribution (P, u-test values were within the range of ± 1.96).

Dose (Gy)	Cells scored	dic-F (No)	Distribution of dicentrics (dic-F)				Yield (Y)	Papworth u test (u test value)	Dispersion index (σ^2/Y)	Distribution
			D0	D1	D2	D3				
0	3036	0	3036	0	0	0	0	0	0	P
0.25	3460	11	3449	11	0	0	0.00318	− 0.13	1	P
0.5	2990	25	2965	25	0	0	0.00836	− 0.32	1	P
1	2660	57	2603	57	0	0	0.02143	− 0.78	0.98	P
2	4596	321	4280	311	5	0	0.06984	− 1.85	0.96	P
3	2227	320	1921	292	14	0	0.14369	− 1.86	0.95	P
4	3350	750	2649	660	33	8	0.22389	− 2.93	0.93	NP (UD)

Table 3. Yield and distribution of dic-F chromosomes involving painted chromosome pairs 1 and 2 following ex vivo irradiation ($n = 3$) with 0–4 Gy of ^{60}Co-γ-rays. Datasets corresponding to 0, 0.25, 0.5, 1, 2, and 3 Gy adhered to the Poisson distribution (P, u-test values were within the range of ± 1.96), whereas the dataset corresponding to 4 Gy exhibited underdispersion (UD, u-test values were outside the range of ± 1.96).

| Dose (Gy)	Cells scored	Acentric fragment (No)	Distribution of acentric-fragments				Yield (Y)	Papworth u test (u test value)	Dispersion index (σ^2/Y)	Distribution
			D0	D1	D2	D3				
0	3036	4	3132	4	0	0	0.00132	− 0.04	1	P
0.25	3460	12	3448	12	0	0	0.00347	− 0.14	0.99	P
0.5	2990	29	2961	29	0	0	0.00969	− 0.37	0.99	P
1	2660	48	2612	48	0	0	0.01805	− 0.65	0.98	P
2	4596	162	4439	152	5	0	0.03525	1.28	1.03	P
3	2227	182	2058	156	13	0	0.08173	2.06	1.06	NP (OD)
4	3350	420	2962	363	18	7	0.12537	2.49	1.06	NP (OD)

Table 4. Yield and distribution of acentric fragments produced from painted chromosome pairs 1 and 2 following ex vivo irradiation ($n = 3$) with 0–4 Gy of ^{60}Co-γ-rays. Datasets corresponding to 0, 0.25, 0.5, 1, and 2 Gy adhered to the Poisson distribution (P, u-test values were within the range of ± 1.96), whereas datasets corresponding to 3 and 4 Gy exhibited overdispersion (OD, u-test values were outside the range of ± 1.96).

β are the linear and quadratic coefficients, respectively. The values of these coefficients are presented in Fig. 2. C represents the background frequency of the aberration in the donor's lymphocytes at the time of blood sampling. The curve fitting parameters for various aberrations, as shown in Fig. 2, demonstrated a good fit to the model.

Comparative evaluation of the yield of BT obtained by two-color, three-color and mFISH
The slides corresponding to irradiation doses of 1 Gy and 2 Gy for volunteer V2 were processed for two-color FISH (Fig. 1), three-color FISH (Fig. 3), and mFISH (Fig. 4) to assess radiation-induced BT frequencies involving chromosome pairs 1 and 2, 1, 2, and 4, and all 24 types of chromosomes, respectively. The results are presented in Table 5.

4
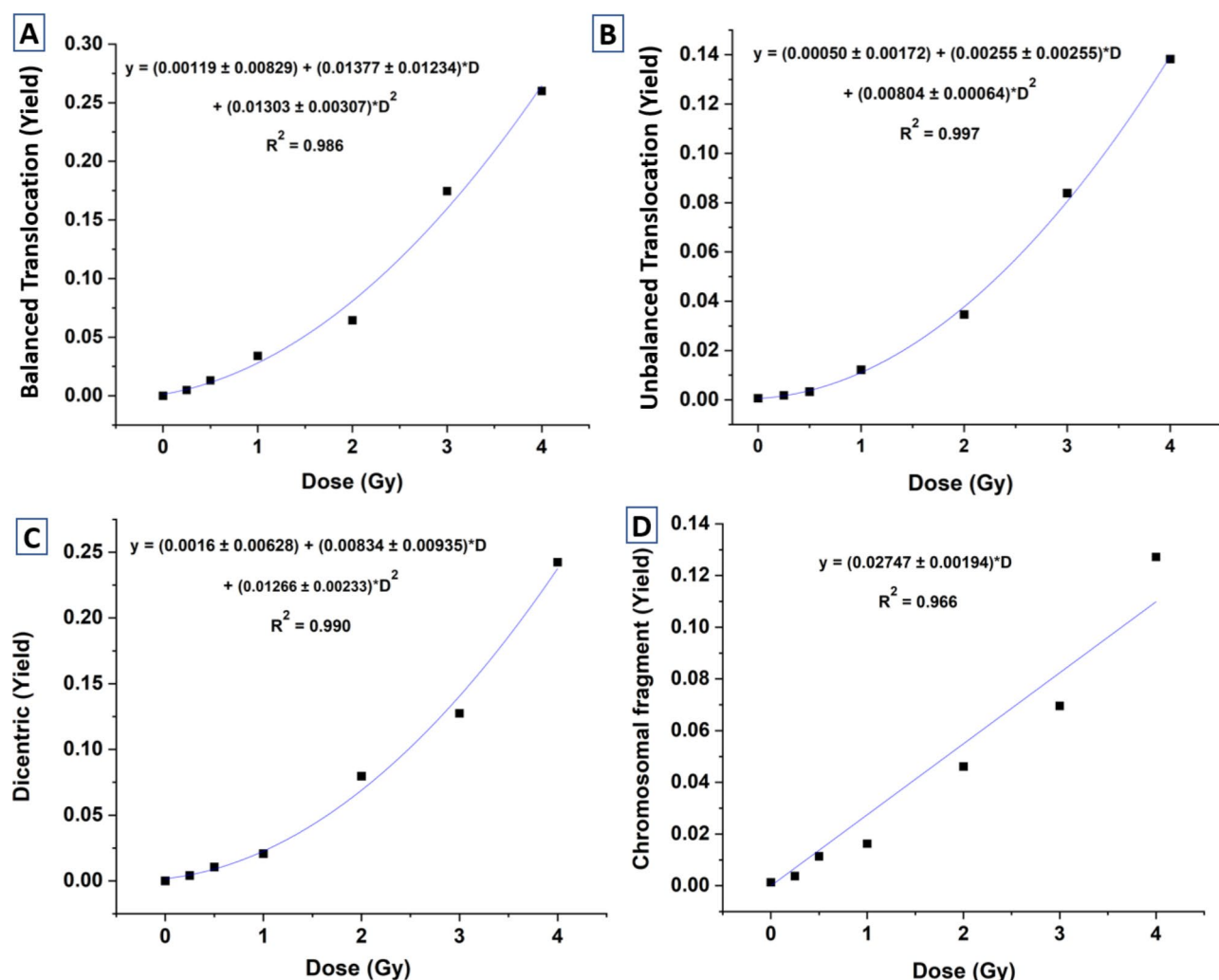
Fig. 1. Dose response curves generated for ^{60}Co-γ-ray-induced (A) BT, (B) UT, (C) dic-F and (D) acentric fragments, scored in the same metaphases processed with FISH, for chromosome pairs 1 and 2.

The variation in BT frequency (genome equivalent) between two-color and three-color FISH was minimal, ranging from + 1.72% to + 4.26%. However, the variation between two-color FISH and mFISH was more pronounced, with values ranging from − 7.33% to + 11.21%. Similarly, the variation between three-color FISH and mFISH exhibited a broader range, from + 7.27% to − 9.21%.

Overall, the variations observed in the BT yield among the three techniques ranged from + 1.72% to + 11.21%, indicating a relatively modest range that falls within the acceptable limits for biodosimetry[6,7].

Comparative evaluation and validation of dose estimation by multiple cytogenetic and protein marker-based assays

Coefficients generated for BT, UT, dic-F, and acentric-fragments in metaphases processed with FISH for chromosome pairs 1 and 2 were used to estimate doses for five blinded samples (BD1–BD5). Additionally, dose estimation for these samples was performed via standard cytogenetic markers, dicentrics and MNs with Giemsa staining, and the DNA double-strand break (DSB) repair protein markers γH2AX and 53BP1 foci. All estimated doses, percent variations, and confidence intervals are presented in Table 6; Fig. 5. In-house established calibration curves were utilized to estimate the doses[17,18,30]. Representative images of the aberrations are shown in Fig. 7.

When the technique-specific average relative errors were compared, individual cytogenetic markers such as BT, UT, dic-F, acentric-fragments, dic-G, and MN presented relative errors in dose estimation ranging from 7 to 32% (Fig. 7). However, the FISH multimarker approach provided significantly improved accuracy, with relative errors ranging from 2 to 7%. When comparing the dose-specific average relative error of the dose estimation, the Avg-FISH method offered more accurate estimates, particularly at lower doses, with average relative errors of 3.2% at 0.25 Gy and 2% at 0.5 Gy. In contrast, independent cytogenetic markers (both FISH and Giemsa stain) presented a significantly greater average relative error of 26% at 0.25 Gy and 19% at 0.5 Gy. Similarly, for higher
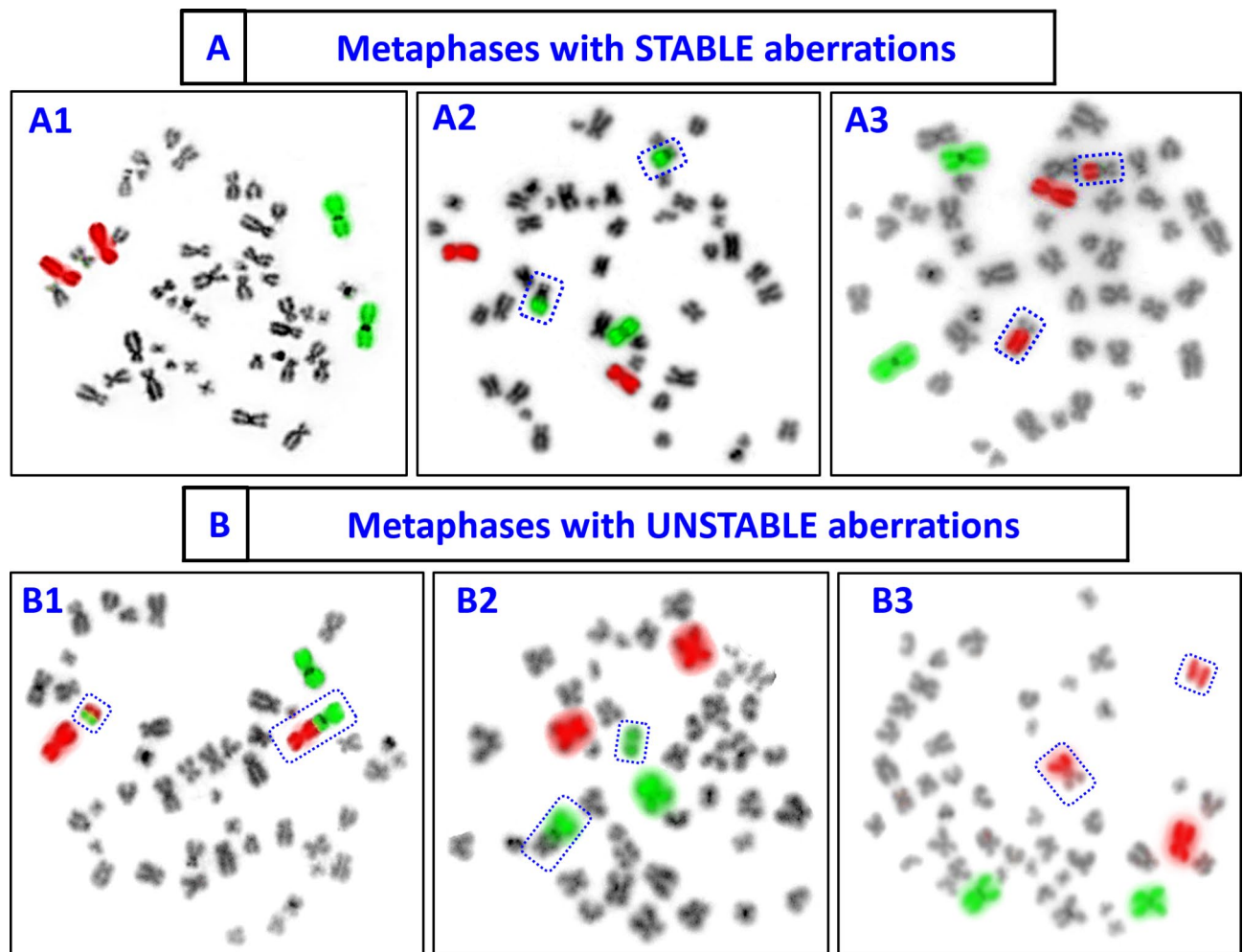
Fig. 2 . Representative metaphase spreads hybridized for two-color FISH. (A) Stable aberrations include (A1) control metaphase (no aberration), (A2) one BT between the green and black chromosomes, and (A3) one BT between the red and black chromosomes. (B) Unstable aberrations consisting of (B1) one dic-F involving green and red chromosomes with a bicolour acentric fragment, (B2) one dic-F involving green and black chromosomes with a bicolour acentric fragment, and (B3) one UT between red and black chromosomes.

doses, the Avg-FISH method provided closer estimates, with average relative errors of 7% at 1 Gy and 4.5% at 2 Gy, compared with 12.7% at 1 Gy and 9.8% at 2 Gy for individual cytogenetic markers.

The analysis of mean dose estimates within ± 25% of the true dose was conducted across all assays. Overall, 90.6% of the dose estimates from the blinded samples fell within this range. The percentages for each blinded dose were as follows: BD1: 100%, BD2: 62.5%, BD3: 100%, BD4: 100%, and BD5: 100%. Notably, the smallest dose (0.25 Gy) resulted in deviations of more than ± 25% across the three assays. However, the Avg-FISH method yielded estimated doses for all five samples within the ± 25% range of their respective true doses.

The mean absolute differences (MADs) between the estimated and true doses were calculated: BT (0.084 Gy), UT (0.098 Gy), dic-F (0.074 Gy), acentric-fragments (0.096 Gy), Avg-FISH (0.036 Gy), dic-G (0.086 Gy), MN (0.130 Gy), γH2AX (0.072 Gy), and 53BP1 (0.064 Gy). Most methods resulted in nearly double the MAD of Avg-FISH, which had the lowest value, indicating superior accuracy. These findings highlight the need for a unified multimarker approach to increase dose precision in biodosimetry and clinical practice.

The protein markers γH2AX and 53BP1 provided the most accurate dose estimates for all blinded samples, except at 2 Gy (BD3). The average relative error ranged from 6 to 12% for γH2AX and 5–10.5% for 53BP1. At lower doses (BD2: 0.25 Gy, BD4: 0.5 Gy), where cytogenetic markers showed greater errors (16–32%), protein markers had more consistent estimates, with 8% error for BD2 and 6–8% for BD4. The greatest amount of error occurred at 2 Gy because the foci overlapped at higher doses. Because they are unstable, protein markers cannot be used after a few days of exposure[17,18].

For sample BD5, the yields of all cytogenetic and protein markers were within the three-sigma range of background frequency, indicating that BD5 is below the detection limits for these assays.
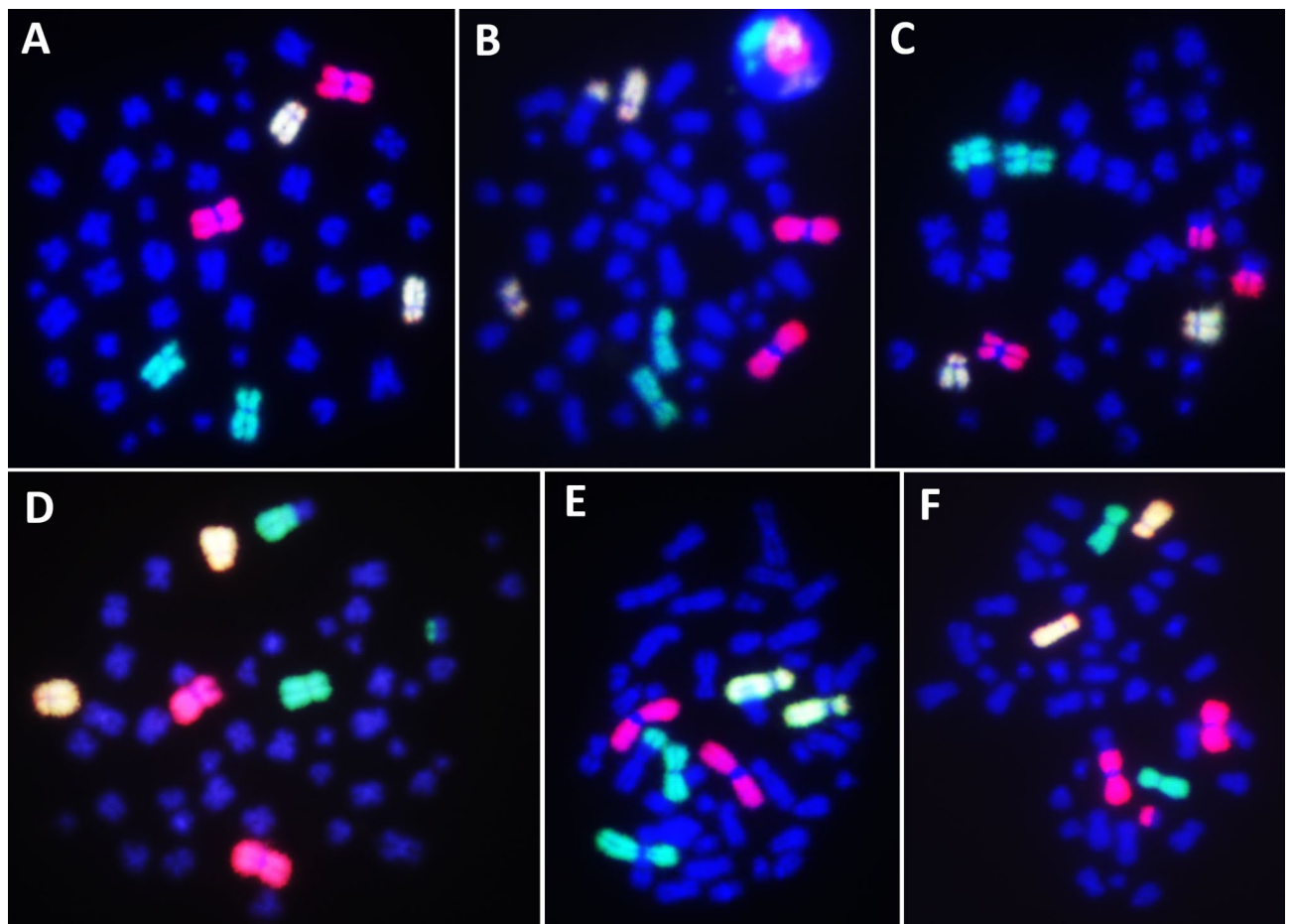
Fig. 3. Representative metaphase spreads hybridized for three-color FISH using whole chromosome paint probes tagged with green (FITC), red (SpO), or a combination of both (FITC and SpO) fluorophores for chromosome pairs 1, 2, and 4. (A) Control metaphase with no aberration. (B) One BT between the yellow and blue chromosomes. (C) One BT between red and blue chromosomes. (D) One BT, between the green and blue chromosomes. (E) One UT between the green and blue chromosomes. (F) One dicentric between the red and blue chromosomes, accompanied by a bicolour acentric fragment. Metaphases with UT (E) and dicentric (F) data were excluded from the scoring.

Discussion

Currently, no single universal marker or detection method is available that can accurately estimate biological doses across all radiation exposure scenarios[6,7]. This limitation arises from significant variations in the stability and detection methods of each cytogenetic marker[31]. However, the FISH-based method has potential as a unified approach. It can differentiate and quantify various cytogenetic markers within the same metaphases, enabling simultaneous detection and assessment of various marker types (Fig. 8)[32]. It can facilitate dosimetry for radiation exposures ranging from recent incidents to those occurring decades ago.

In this study, dose−response curves were established for ^{60}Co-γ-ray-induced BT, UT, dic-F and acentric-fragments, which were all quantified from the same metaphases. This comprehensive approach eliminates the need for marker-specific methods, reduces interexperimental variations, and facilitates multimarker dose assessment. According to the IAEA and ISO recommendations, the most precise dose estimations rely on multimarker-based assessments, where the maximum possible number of markers accounts for accurate dose reconstruction[6,7].

Although multimarker dose assessment is the preferred approach for radiation dose estimation, its applicability varies with the circumstances of exposure. Different cytogenetic markers have specific strengths and limitations. BTs are stable aberrations formed by balanced exchanges between chromosomes without loss of genetic information[33]. They are suitable for (but not limited to) biodosimetry of past and cumulative exposures, enabling long-term dose assessments, including lifetime monitoring for regulatory purposes in radiation workers[34]. UT and DC; these unstable aberrations are effective for dosimetry of recent exposures, typically within a few months postexposure[6,7]. Acentric-fragments, while not highly specific to radiation, it can still be useful as secondary markers in recent exposure assessments when combined with other cytogenetic markers[35].

FISH enables the quantification of various chromosomal aberrations, facilitating the selection of markers for assessing radiation exposure, whether recent or past, and for estimating both current and cumulative doses,
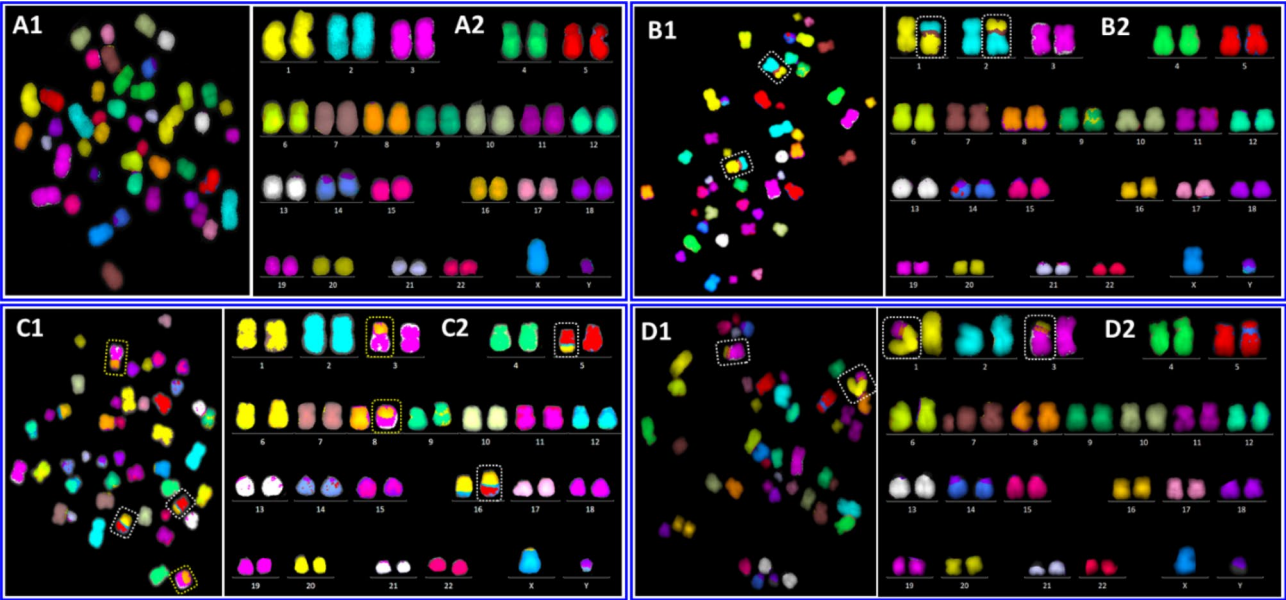
Fig. 4. Representative metaphase spreads hybridized with mFISH (24-color FISH), where all 24 chromosome types were labeled with distinct colors. Metaphases exhibit (A) control with no aberration, (B) one BT between chromosomes 1 and 2, (C) two BTs between chromosomes 3 and 8 and between chromosomes 5 and 16, and (D) one BT between chromosomes 1 and 3, accompanied by an acentric fragment from chromosome 7.

	Two color FISH (Chromosome pair 1 & 2 were painted)		Three color FISH (Chromosome pair 1, 2 & 4 were painted)		mFISH (All 24 types of chromosomes were painted)	Variation (%)		
Dose (Gy)	Yield of BT (F_P)	Frequency genome equivalent (F_G)	Yield of BT (F_P)	Frequency genome equivalent (F_G)	Whole genome BT frequency (mFISH)	Between two and three color FISH	Between two color and mFISH	Between three color and mFISH
1	0.0298 (~ 2300 cells analyzed)	0.1034	0.0356 (~ 1200 cells analyzed)	0.0990	0.0918 (~ 200 cells analyzed)	+ 4.26%	+ 11.21%	+ 7.27%
2	0.0749 (~ 2300 cells analyzed)	0.2675	0.0946 (~ 1000 cells analyzed)	0.2629	0.2871 (~ 100 cells analyzed)	+ 1.72	− 7.33%	− 9.21

Table 5. Comparative assessment of two-color, three-color, and mFISH for detecting BT at 1 Gy and 2 Gy. Genome-equivalent translocation frequencies were calculated via a modified Lucas formula for both two-color and three-color FISH techniques.

all from a single sample. In contrast, the Giemsa staining method requires meticulous sample preparation and relies on the expertise of skilled personnel to accurately identify chromosomal aberrations. This method carries a significant risk of missing crucial aberrations, whereas FISH has much greater accuracy and sensitivity, with detection limits for chromosomal translocations being approximately 1000-fold better than those of Giemsa-based methods[6,7,33].

To test compliance with the Poisson distribution, the dispersion index (σ^2/Y) and the Papworth u-test were thoroughly examined for all aberrations (Tables 1, 2, 3 and 4). Ideally, for the aberration distribution to adhere to the Poisson distribution, the dispersion index (σ^2/Y) should be approximately one, and the u-test value should fall within the range of ± 1.96 for each dose point[36]. BT, UT and DF-F adhered to the Poisson distribution for all dose points, except for one (4 Gy in dic-F), whereas acentric fragments adhered at lower doses but deviated at higher doses (3 and 4 Gy) (Tables 1, 2, 3 and 4). Underdispersion in the distribution of dicentric at high doses has been reported by several authors[37–39]. In this study, underdispersion was observed at the highest dose point (4 Gy). We compared the observed dicentric distribution with the Poisson model (Tables 3 and 4), which revealed fewer cells without dicentrics or with low dicentric counts than expected, with a notably lower number of cells without aberrations, than anticipated. A plausible explanation could be linked to the repair dynamics of DSBs. It has been reported that the likelihood of correct or incorrect DSB rejoining depends on the spatial and temporal proximity of DSBs[40,41]. At high doses, where DSBs are more frequent, the increased likelihood of misrejoining may lead to an excess of cells with higher dicentric counts, thereby reducing the proportion of cells with zero or few dicentrics and contributing to underdispersion at 4 Gy[42]. Higher doses (3 and 4 Gy) may also induce

Dose blinded sample	True dose (Gy)	Dose estimation by two color FISH (involving chromosome pair 1 and 2)										Dose estimation by Giemsa stained dic-G and MN				Dose estimation by γH2AX and 53BP1 Immunofluorescence			
		Estimated dose by BT	Relative error of the dose estimate (%)	Estimated dose by UT	Relative error of the dose estimate (%)	Estimated dose by dic-F	Relative error of the dose estimate (%)	Estimated dose by Acentric Fragment	Relative error of the dose estimate (%)	Average dose estimated by FISH based markers	Relative error of the dose estimate (%)	Estimated dose by dic-G	Relative error of the dose estimate (%)	Estimated dose by MN	Relative error of the dose estimate (%)	Estimated dose by γH2AX	Relative error of the dose estimate (%)	Estimated dose by 53BP1	Relative error of the dose estimate (%)
BD1	1	1.1 Gy [95% CI: 0.84–1.39]	+10	1.12 Gy [95% CI: 0.78–1.51]	+12	0.91 Gy [95% CI: 0.62–1.22]	−9	1.14 Gy [95% CI: 0.96–1.33]	+14	1.07 Gy	+7	1.12 Gy [95% CI: 1.0–1.24]	+13	0.82 Gy [95% CI: 0.70–0.95]	−18	0.94 Gy [95% CI: 0.82–1.06]	−6	1.05 Gy [95% CI: 0.97–1.13]	+5
BD2	0.25	0.20 Gy [95% CI: 0.03–0.46]	−24	0.32 Gy [95% CI: 0–0.7]	+28	0.18 Gy [95% CI: 0.01–0.42]	−20	0.33 Gy [95% CI: 0.1–0.55]	+32	0.258 Gy	+3.2	0.20 Gy [95% CI: 0.09–0.33]	−24	0.18 Gy [95% CI: 0.1–0.28]	−28	0.27 Gy [95% CI: 0.24–0.31]	+8	0.27 Gy [95% CI: 0.25–0.29]	+8
BD3	2	1.82 Gy [95% CI: 1.45–2.23]	−9	1.78 Gy [95% CI: 1.44–2.15]	−11	1.86 Gy [95% CI: 1.58–2.16]	−7	2.16 Gy [95% CI: 1.99–2.34]	+8	1.91 Gy	−4.5	1.82 Gy [95% CI: 1.65–2.0]	−9	1.71 Gy [95% CI: 1.51–1.91]	−14.5	1.75 Gy [95% CI: 1.52–1.97]	−12.5	1.79 Gy [95% CI: 1.65–1.93]	−10.5
BD4	0.5	0.59 Gy [95% CI: 0.35–0.87]	+18	0.42 Gy [95% CI: 0.04–0.87]	−16	0.57 Gy [95% CI: 0.23–0.92]	+22	0.4 Gy [95% CI: 0.19–0.62]	−20	0.49 Gy	−2	0.58 Gy [95% CI: 0.47–0.71]	+16	0.61 Gy [95% CI: 0.5–0.73]	+22	0.53 Gy [95% CI: 0.46–0.59]	+6	0.54 Gy [95% CI: 0.49–0.58]	+8
BD5	0	0 Gy [95% CI: 0.0–0.0]	0.0	0 Gy [95% CI: 0.0–0.0]	0.0	0 Gy [95% CI: 0.0–0.0]	0.0	0 Gy [95% CI: 0.0–0.0]	0.0	0 Gy	0.0	0 Gy [95% CI: 0.0–0.0]	0.0	0 Gy [95% CI: 0.0–0.0]	0.0	0 Gy [95% CI: 0.0–0.0]	0.0	0 Gy [95% CI: 0.0–0.0]	0.0

Table 6. Dose estimation for five blinded samples (BD1 to BD5) via BT, UT, dic-F, acentric-fragments, and Avg-FISH in metaphases processed with two-color FISH, utilizing coefficients generated in this study. Additionally, doses were estimated via independent methods: dic-G, MN (Giemsa-stained), γH2AX (immunofluorescence-stained), and 53BP1 (immunofluorescence-stained), employing previously established coefficients. The results of Avg-FISH were compared with those obtained via independent methods.
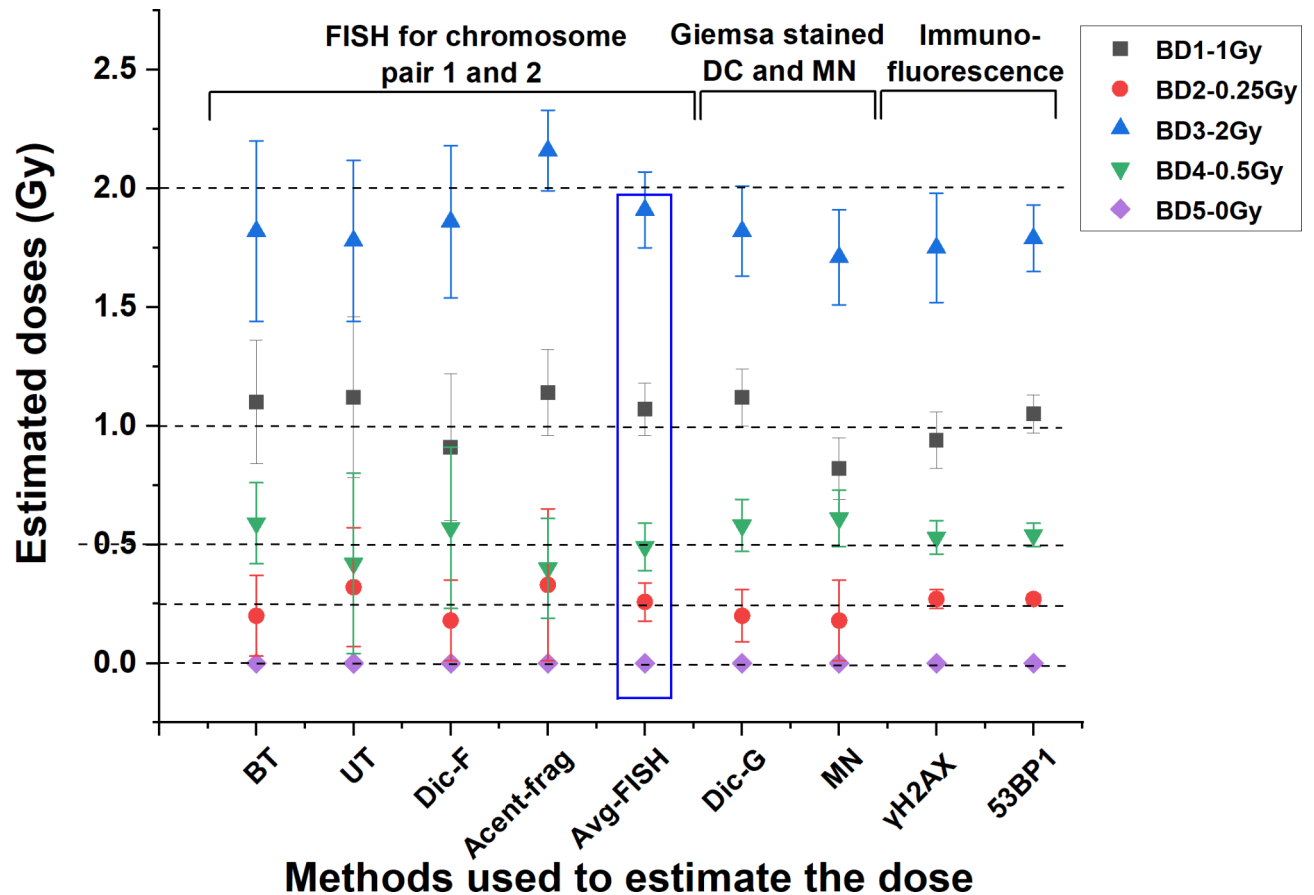
Fig. 5. Dose estimation for five blinded samples (BD1-BD5) via various cytogenetic markers. Doses were measured by quantifying yields from BT, UT, dic-F, Fr, and Avg-FISH in metaphases processed with two-color FISH. Additional estimates were obtained via independent methods: dic-G, MN analysis of binucleated Giemsa-stained cells, and immunofluorescence detection of γH2AX and 53BP1 foci in G0 lymphocytes.

complex chromosomal lesions, complicating characterization and introducing uncertainties[43,44]. Additionally, lower detection sensitivity at higher doses may lead to the underestimation of chromosomal aberrations.

In this study, DRCs were generated by assessing chromosomal aberrations via two-color FISH on chromosome pairs 1 and 2, which covered 16.32% of the genome. This method was compared with three-color FISH (22.71% of the genome) and mFISH (100%). The comparative evaluation for biodosimetry revealed minimal variation (+1.72% to +4.26%) in BT yield between two-color and three-color FISH but a significant difference (−9.21% to +11.21%) compared with mFISH. This variation suggests that the frequency of BT may not align with chromosome size, which was assumed in the Lucas formula[6,7]. For routine or regulatory biodosimetry, practical concerns favor two-color or three-color FISH owing to shorter processing times, less specialized instrumentation, lower probe costs, and reduced expertise demands. However, mFISH offers a distinct advantage in the analysis of interchromosomal alterations across all 24 human chromosomes, particularly in cases of complex rearrangements. Its high-resolution capabilities enable the identification of rare chromosomal events and intricate rearrangements that may be challenging to detect via two- or three-color FISH[45–47].

The established dose−response curves were validated by reconstructing the doses of 5 blinded samples. The FISH multimarker approach consistently showed better accuracy than individual cytogenetic markers (both FISH and Giemsa staining), with significantly lower relative errors, especially at low doses. For example, the average relative error of the Avg-FISH method was 3.2% at 0.25 Gy and 2% at 0.5 Gy, whereas the average relative error was much greater for individual markers (16–32%). At higher doses, the Avg-FISH method also showed improved accuracy. Overall, 95% of the dose estimates were within ± 25% of the true dose across assays; however, the multimarker FISH offered 100% doses within ± 25% of the true doses, indicating robust precision. MAD further exhibited superior accuracy to the Avg-FISH method, with 2.1–3.6 times lower deviations than those of other individual techniques (FISH and Giemsa staining). Protein markers (γH2AX, 53BP1) also provided reliable estimates, especially at lower doses, although some challenges arose at higher doses. This underestimation of doses at higher doses may be attributed to the overlapping of foci, which can hinder accurate quantification and lead to a reduced detection of individual foci[48,49].

Overall, our findings emphasize the implementation of a multimarker approach in radiation biodosimetry to increase the precision and accuracy of dose estimation, thereby facilitating improved management and treatment decisions for radiation-exposed individuals. In addition, the multimarker strategy could have significant
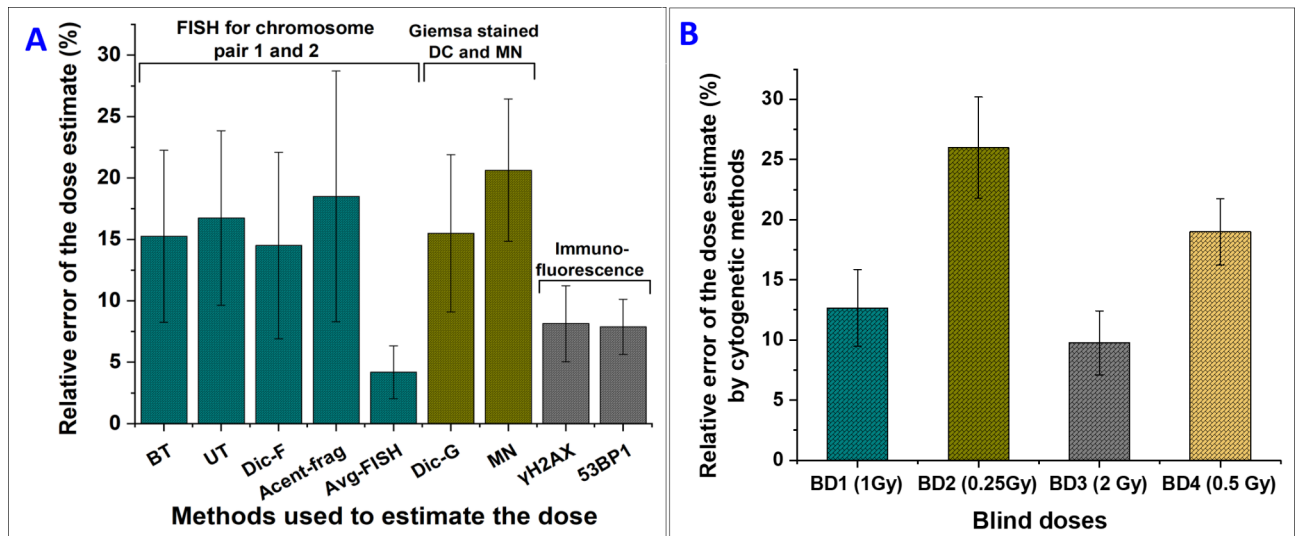
Fig. 6. (A) Relative error (%) in dose estimates from BT, UT, dic-F, acentric fragment, and Avg-FISH using the unified two-color FISH method compared with independent methods: dic-G, MN (Giemsa-stained), γH2AX foci (immunofluorescence), and 53BP1 foci (immunofluorescence). (B) Relative error (%) for blinded samples (BD1 to BD4). Higher doses (BD1–1 Gy and BD3–2 Gy) resulted in more accurate estimates, whereas lower doses (BD2–0.25 Gy and BD4–0.5 Gy) resulted in greater deviations. The variation in the estimated doses was ranked as follows: BD3<BD1<BD4<BD2. All cytogenetic methods (BT, UT, dic-F, acent-frag, DC, MN) were considered in the analysis.

implications in radiation therapy, enabling clinicians to more accurately estimate radiation doses and optimize treatment plans for patients undergoing radiological treatments.

While the study's direct applications are evident, it is important to acknowledge its limitations as well. All the dose–response curves were generated ex vivo and require in vivo validation. However, ex vivo response curves in other studies have aligned well with in vivo data, and these curves can be further validated through interlaboratory comparisons using dose-blinded samples. A comprehensive database of calibration curves for diverse populations and radiation conditions would broaden the applicability of these methods across different radiological incidents and clinical scenarios. The limited applicability of current methods in extreme or complex radiation exposure scenarios (e.g., mixed radiation fields, post-nuclear accidents) is an area where additional research is needed. Further studies should explore integrating other biomarkers or technological advancements to increase the sensitivity and specificity of dosimetry in such settings.

Conclusion

This study established calibration curves for chromosomal aberrations such as BT, UT, dic-F, and acentric fragments via two-color FISH to quantify markers for both recent and cumulative radiation dosimetry from the same sample. Compared with the Giemsa-stained methods, the multimarker FISH approach (Avg-FISH) significantly improved accuracy and consistency, reducing dose estimation errors by 3.7–4.9 times. A comparison of two-color, three-color, and mFISH revealed minimal variation between the two- and three-color methods, with mFISH showing slightly greater deviations. Owing to their simplicity and lower cost, two-color and three-color FISH provide practical advantages for routine biodosimetry. Validation with blinded samples confirmed the precision of Avg-FISH, which achieved minimal average error in dose estimation over individual markers. This study demonstrated the effectiveness of the multimarker FISH method in providing precise dose estimations and selecting appropriate markers for different exposure scenarios, making it highly versatile for both immediate and retrospective biodosimetry.
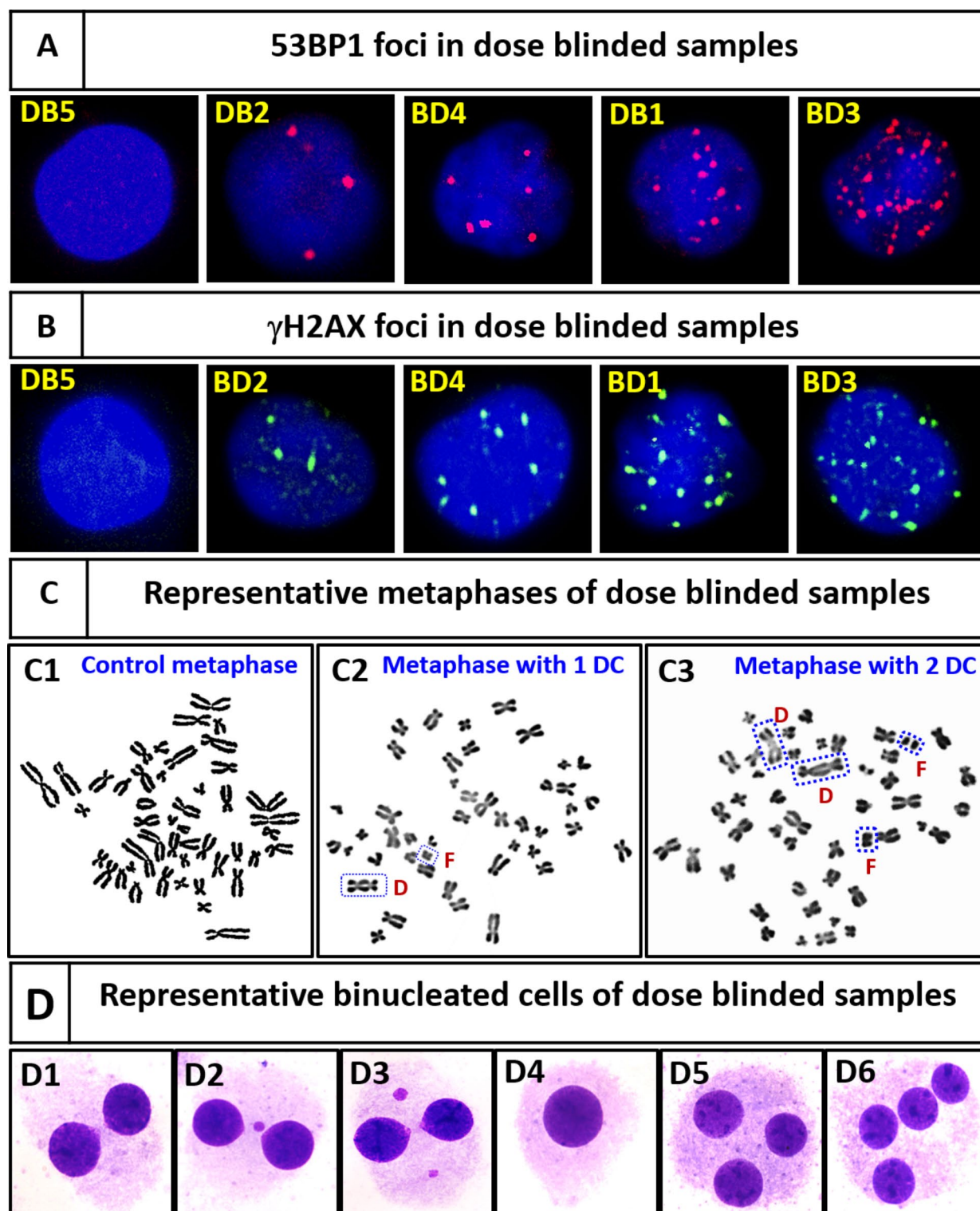
Fig. 7. (A & B) Representative G0 lymphocytes from samples BD5, BD2, BD4, BD1, and BD3, illustrating the respective numbers of 53BP1 (red) and γH2AX (green) foci observed after 1 h of incubation postirradiation under optimal conditions. (C) Representative metaphases: (C1) control with no dic, (C2) one dic with an acentric fragment, and (C3) two dic with two acentric fragments. (D) Representative binucleated lymphocytes: (D1) control with no MNs, (D2) one MN, (D3) two MNs, (D4) mononucleated lymphocytes, (D5) trinucleated lymphocytes, and (D6) tetranucleated lymphocytes. Mononucleated, trinucleated, and tetranucleated lymphocytes were excluded from the dose estimations.
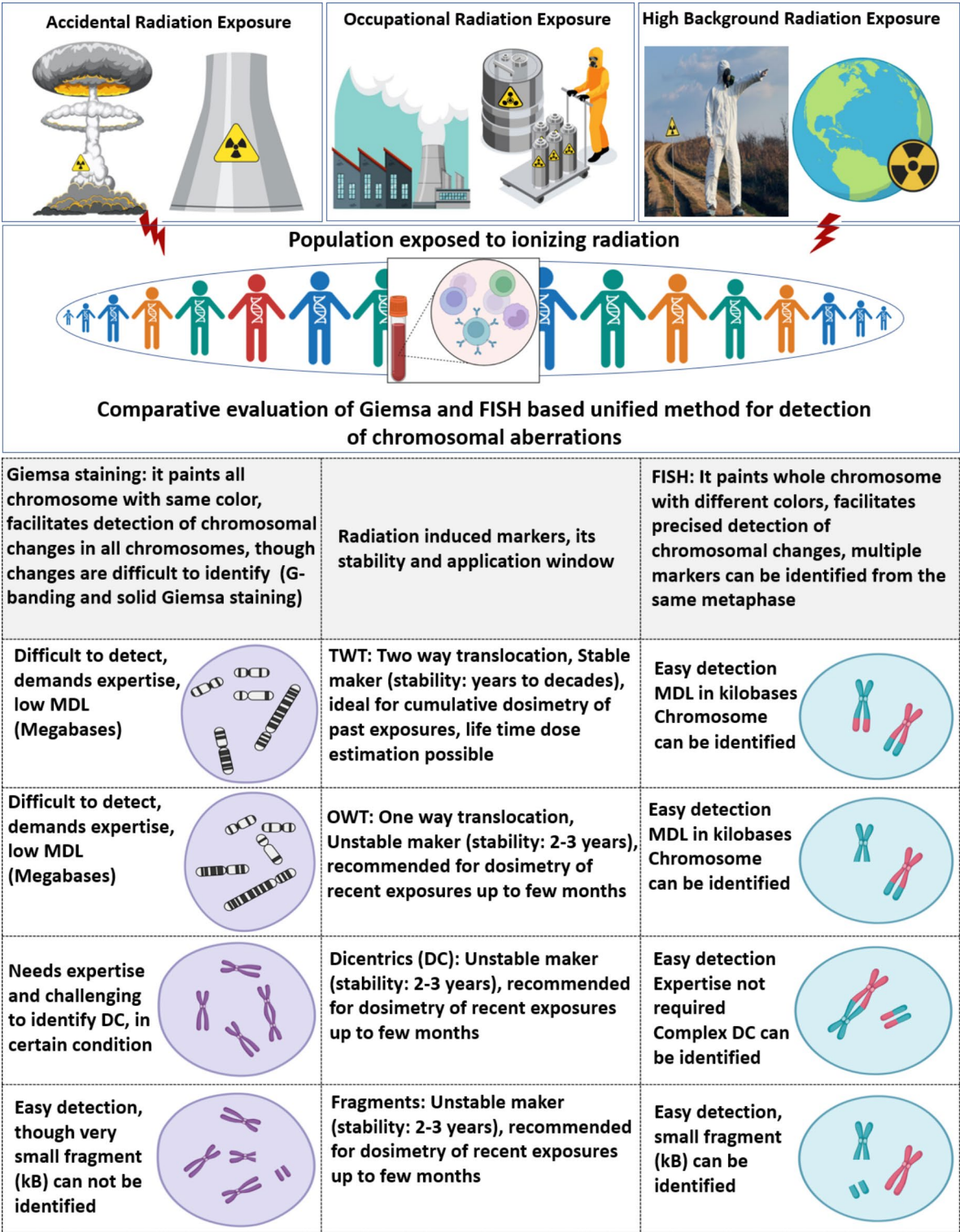
Fig. 8. Graphical summary of comparative evaluation of Giemsa and FISH-based methods for detection of various chromosomal aberrations in biodosimetric applications.

Data availability

All data generated or analysed during this study are included in this published article.

References

1. Henriksen, T. & Maillie, D. H. *Radiation and Health* (CRC, 2002).
2. Shahbazi-Gahrouei, D., Gholami, M. & Setayandeh, S. A review on natural background radiation. *Adv. Biomed. Res.* **2**(1), 65 (2013).
3. Chaurasia, R. K., Sapra, B. K. & Aswal, D. K. *Interplay of Immune Modulation, Adaptive Response and Hormesis: Suggestive of Threshold for Clinical Manifestation of Effects of Ionizing Radiation at low Doses?* 170178 (Science of The Total Environment, 2024).
4. Frane, N. & Bitterman, A. *Radiation Safety and Protection* (Wiley, 2020).
5. Izewska, J. & Rajan, G. *Radiation Dosimeters. Radiation Oncology Physics: A Handbook for Teachers and Students* 71–99 (2005).
6. IAEA, C. D. *Applications in Preparedness for and Response to Radiation Emergencies* (EPR-Biodosimetry. International Atomic Energy Agency, 2011).
7. ISO. *ISO 19238:2023 Radiological Protection—Performance Criteria for Service Laboratories Performing Biological Dosimetry by cytogenetics—Dicentric Assay* (International Organization for Standardization, 2023).
8. Bhavani, M. et al. Dicentric chromosome aberration analysis using giemsa and centromere specific fluorescence in-situ hybridization for biological dosimetry: an inter-and intra-laboratory comparison in Indian laboratories. *Appl. Radiat. Isot.* **92**, 85–90 (2014).
9. Selvan, G. T. & Venkatachalam, P. Potentials of cytokinesis blocked micronucleus assay in radiation triage and biological dosimetry. *J. Genet. Eng. Biotechnol.* **22**(4), 100409 (2024).
10. Roukos, V. & Misteli, T. The biogenesis of chromosome translocations. *Nat. Cell Biol.* **16**(4), 293–300 (2014).
11. 11. ISO 20046:2019(en) Radiological protection—performance criteria for laboratories using Fluorescence In Situ Hybridization (FISH) translocation assay for assessment of exposure to ionizing radiation (2024).
12. Haskins, J. S. & Kato, T. A. Reciprocal translocation analysis with whole chromosome painting for FISH. *Radiat. Cytogenet. Methods Protocols* **2019**, 117–122. (2019).
13. Bezrookove, V. et al. Individuals with abnormal phenotype and normal G-banding karyotype: improvement and limitations in the diagnosis by the use of 24-colour FISH. *Hum. Genet.* **106**, 392–398 (2000).
14. de Lemos Pinto, M. M. P., Santos, N. F. G. & Amaral, A. Current status of biodosimetry based on standard cytogenetic methods. *Radiat. Environ. Biophys.* **49**, 567–581 (2010).
15. Edwards, A. A., Lloyd, D. C. & Szłuińska, M. Retrospective biological dosimetry by FISH. *Chromosom. Alterat. Methods Results Importance Hum. Health* **2007**, 371–380 (2007).
16. Tolstykh, E. I., Degteva, M. O., Vozilova, A. V. & Anspaugh, L. R. Local bone-marrow exposure: how to Interpret the data on stable chromosome aberrations in circulating lymphocytes? (some Comments on the use of FISH Method for dose Reconstruction for Techa Riverside Residents). *Radiat. Environ. Biophys.* **56**, 389–403 (2017).
17. Chaurasia, R. K., Shirsath, K. B., Desai, U. N., Bhat, N. N. & Sapra, B. K. Establishment of in vitro calibration curve for 60Co-γ-rays induced phospho-53BP1 foci, rapid biodosimetry and initial triage, and comparative evaluations with γH2AX and cytogenetic assays. *Front. Public Health* **10**, 845200 (2022).
18. Chaurasia, R. K. et al. Establishment and multiparametric-cytogenetic validation of 60Co-gamma-ray induced, phospho-gamma-H2AX calibration curve for rapid biodosimetry and triage management during radiological emergencies. *Mutation Res. Genet. Toxicol. Environ. Mutagenesis* **866**, 503354 (2021).
19. Vijayalakshmi, J. et al. Lab to emergency: establishment and validation of automated method for rapid biodosimetry, 09 May 2024, PREPRINT (Version 1) available at Research Square. https://doi.org/10.21203/rs.3.rs-4380326/v1 (2024).
20. Vijayalakshmi, J. et al. Establishment of ex vivo calibration curve for X-ray induced dicentric + ring and micronuclei in human peripheral lymphocytes for biodosimetry during radiological emergencies, and validation with dose blinded samples. *Heliyon* **9**, 6 (2023).
21. Krishnaja, A. P. & Sharma, N. K. Transmission of γ-ray-induced unstable chromosomal aberrations through successive mitotic divisions in human lymphocytes in vitro. *Mutagenesis* **19**(4), 299–305 (2004).
22. Chaurasia, R. K., Shirsath, K. B. & Sapra, B. K. Protocol for one-step selective lysis of red blood cells and platelets with long-term preservation of white blood cells (human) at ambient temperature. *STAR Protocols* **2**(4), 100834 (2021).
23. Sotnik, N. V., Osovets, S. V., Scherthan, H. & Azizova, T. V. mFISH analysis of chromosome aberrations in workers occupationally exposed to mixed radiation. *Radiat. Environ. Biophys.* **53**, 347–354 (2014).
24. Lucas, J. N. et al. Rapid translocation frequency analysis in humans decades after exposure to ionizing radiation. *Int. J. Radiat. Biol.* **62**(1), 53–63 (1992).
25. Szluinska, M., Edwards, A. A. & Lloyd, D. C. *Statistic Methods for Biological Dosimetry, Health Protection Agency. HPA–RPD–011* (Chilton, 2005).
26. Alsbeih, G. A., Al-Hadyan, K. S., Al-Harbi, N. M., Judia, S. S. B. & Moftah, B. A. Establishing a reference dose–response calibration curve for dicentric chromosome aberrations to assess accidental radiation exposure in Saudi Arabia. *Front. Public. Health* **2020**, 8 (2020).
27. Coleman, C. N. & Koerner, J. F. Biodosimetry: medicine, science, and systems to support the medical decision-maker following a large scale nuclear or radiation incident. *Radiat. Prot. Dosimetry*. **172**(1–3), 38–46 (2016).
28. International Organization for Standardization (ISO). Radiation protection–performance criteria for service laboratories performing biological dosimetry by cytogenetics. Geneva: ISO, 19238, 2014 (2004).
29. Orji, E. I. et al. Reducing errors in slope in physics graphs using origin lab software. *Webology* **19**, 3 (2022).
30. Bhat, N. N., Anjaria, K. B. & Rao, B. S. Dose rate effect and its implications in biodosimetry using chromosomal aberration analysis. *Radiat. Prot. Environ.* **26**(3–4), 536–540 (2003).
31. Swartz, H. M., Williams, B. B. & Flood, A. B. Overview of the principles and practice of biodosimetry. *Radiat. Environ. Biophys.* **53**, 221–232 (2014).
32. Lomonosova, E. E. et al. The three-color FISH method: a comparison of retrospective cytogenetic dose estimations in four patients who underwent acute accidental irradiation. *Biology Bull.* **50**(12), 3278–3285 (2023).
33. Lucas, J. N. & Deng, W. Our views on issues in radiation biodosimetry based on chromosome translocations measured by FISH. *Radiat. Prot. Dosimetry*. **88**(1), 77–86 (2000).
34. Tolstykh, E. I., Vozilova, A. V., Degteva, M. O. & Akleyev, A. V. Dependence of the translocation frequency in blood lymphocytes on the dose and age at the onset of exposure in residents of the Techa riverside settlements. *Biol. Bull.* **50**(12), 3184–3195 (2023).
35. Ludovici, G. M. et al. Cytogenetic bio-dosimetry techniques in the detection of dicentric chromosomes induced by ionizing radiation: a review. *Eur. Phys. J. Plus* **136**(5), 482 (2021).
36. Szłuińska, M., Edwards, A. A. & Lloyd, D. C. Statistical methods for biological dosimetry. In *Chromosomal Alterations: Methods, Results and Importance in Human Health* 351–370 (Springer, 2007).
37. Edwards, A. A., Lloyd, D. C. & Purrott, R. J. Radiation induced chromosome aberrations and the Poisson distribution. *Radiat. Environ. Biophys.* **16**(2), 89–100 (1979).
38. Yao, B. et al. Biological dose estimation for two severely exposed patients in a radiation accident in Shandong Jining, China, in 2004. *Int. J. Radiat. Biol.* **86**(9), 800–808 (2010).
39. Vinnikov, V. A. & Maznyk, N. A. Cytogenetic dose-response in vitro for biological dosimetry after exposure to high doses of gamma-rays. *Radiat. Prot. Dosimetry* **154**(2), 186–197 (2013).
40. Rothkamm, K., Gunasekara, K., Warda, S. A., Krempler, A. & Löbrich, M. Radiation-induced HPRT mutations resulting from misrejoined DNA double-strand breaks. *Radiat. Res.* **169**(6), 639–648 (2008).

41. Kühne, K., Rothkamm, M. & Löbrich, M. No dose-dependence of DNA double-strand break misrejoining following α-particle irradiation. *Int. J. Radiat. Biol.* **76**(7), 891–900 (2000).
42. Pujol, M. et al. A new model of biodosimetry to integrate low and high doses. *PLoS One* **9**(12), e114137 (2014).
43. Foray, N., Charvet, A. M., Duchemin, D., Favaudon, V. & Lavalette, D. The repair rate of radiation-induced DNA damage: a stochastic interpretation based on the gamma function. *J. Theor. Biol.* **236**(4), 448–458 (2005).
44. Georgakilas, A. G., O'Neill, P. & Stewart, R. D. Induction and repair of clustered DNA lesions: what do we know so far? *Radiat. Res.* **180**(1), 100–109 (2013).
45. Hande, M. P. et al. Complex chromosome aberrations persist in individuals many years after occupational exposure to densely ionizing radiation: an mFISH study. *Genes Chromosom. Cancer* **44**(1), 1–9 (2005).
46. Shibata, F. & Hizume, M. Multi-color fluorescence in situ hybridization. *Cytologia* **80**(4), 385–392 (2015).
47. Shakoori, A. R. Fluorescence in situ hybridization (FISH) and its applications. *Chromosome Struct. Aberrations* **2017**, 343–367 (2017).
48. Horn, S., Barnard, S. & Rothkamm, K. Gamma-H2AX-based dose estimation for whole and partial body radiation exposure. *PloS One* **6**(9), e25113 (2011).
49. Wanotayan, R. et al. Quantification of histone H2AX phosphorylation in white blood cells induced by ex vivo gamma irradiation of whole blood by both flow cytometry and foci counting as a dose estimation in rapid triage. *Plos One* **17**(3), e0265643 (2022).

Acknowledgements

Author contributions

R.K. Chaurasia, N.N. Bhat, A. Khan and B.K. Sapra, contributed to the study conception and design. Material preparation, data collection and analysis were performed by R.K. Chaurasia, K.B. Shirsath, U.S. Mungse, N.N. Bhat, A. Khan and B.K. Sapra. The first draft of the manuscript was written by R.K. Chaurasia and all authors commented on previous versions of the manuscript. All authors read and approved the final manuscript.

Funding

Competing interests

The authors declare no competing interests.

Ethics statement

This study was performed in accordance with the principles of the Declaration of BARC ethical committee. Approval was granted by institutional ethical committee of Bhabha Atomic Research Centre.

Additional information

Correspondence and requests for materials should be addressed to B.K.S.

Reprints and permissions information is available at www.nature.com/reprints.

Publisher's note Springer Nature remains neutral with regard to jurisdictional claims in published maps and institutional affiliations.